The Transmission of Rossby Waves through Basin Barriers*

JOSEPH PEDLOSKY

Physical Oceanography Department, Woods Hole Oceanographic Institution, Woods Hole, Massachusetts

(Manuscript received 17 November 1998, in final form 16 February 1999)

ABSTRACT

The response of a basin with a topographic barrier to spatially localized and time periodic forcing is considered. The barrier, which almost completely divides the full basin into two adjacent subbasins, is offered as a model of either a planetary island in the wind-driven circulation or a portion of the midocean ridge in the abyssal circulation.

The barrier completely blocks the flow between the two adjacent subbasins except for the possibility of flow through two small gaps at the termini of the barrier. The barrier has nonzero thickness, and scale-dependent lateral friction acts in the gap channels to impede the flow from one subbasin to the next. Bottom friction also acts uniformly on the flow in the basin. The degree to which localized forcing is able to excite large-scale motions in the adjacent subbasin is shown to be connected to the structure of the forcing and its frequency.

In the absence of forcing and friction a set of full basin normal modes exist. The degree to which the forcing is able to resonate with such modes determines the degree to which energy can be transmitted from one subbasin to the other. Friction in the gaps reduces both the amplitude of that transmission and smooths the peaks of the response curve of the motion as a function of frequency in both subbasins. However, even for substantial friction, a considerable amount of large-scale variability can be excited in the adjacent basin. The quantitative dependence of the response on the degree of friction, the length of the channels representing the gaps, and the meridional structure of the forcing are discussed.

In cases where the western boundary of the basin is nonreflecting, so that no full basin normal modes are possible, substantial energy transmission is still demonstrated. Whether resonance occurs or not, the necessity for energy transmission is closely related to the existence of the integral circulation constraint around the island barrier and the possibility of resonance acts mainly to set the level of the response.

1. Introduction

In a recent paper (Pedlosky and Spall 1999, hereafter PS), the Rossby beta-plane normal modes were studied in a basin very nearly separated into two distinct subbasins by a long, thin meridional barrier. The two subbasins were allowed to communicate only through very narrow gaps in the barrier. The study was motivated by the results of numerical experiments carried out by Spall and described in PS. Briefly, the calculations showed instabilities of baroclinic type that grew on the mean flow generated by steady forcing in a two-layer model. The instabilities were of relatively small scale, of the order of the deformation radius, but it was observed that basin-scale variability was present in both subbasins apparently excited by the small-scale instabilities localized on the eastern side of the barrier. In some manner, the naturally generated variability on one side of the barrier is able to communicate to the other subbasin and excite large-scale oscillations there. We thought of the basic model as an idealization of the circulation around planetary-scale islands or equally apt, as the circulation of abyssal waters around and through the large-scale midocean ridge systems with their gaps. Our preliminary work on the steady-state problem has been reported in Pedlosky et al. (1998).

It seemed to us that the first step in understanding the ability of time-dependent oscillations to be excited across the narrow gaps separating the subbasins was to examine the possible Rossby wave normal modes that could exist in such geometries. We were well aware of the heavy idealization of the total problem involved in searching for inviscid normal modes, but we felt it was illuminating as a first step in understanding how basin-scale oscillations could be transmitted through such narrow passageways.

The key feature of the problem that helped understand the process of transmission was the presence of the integral constraint of conservation of circulation around the island. For periodic, inviscid motions, the constraint

* Woods Hole Oceanographic Institution Contribution 9874.

Corresponding author address: Dr. Joseph Pedlosky, Physical Oceanography Department, Woods Hole Oceanographic Institution, Woods Hole, MA 02543.
E-mail: jpedlosky@whoi.edu

reduces to the statement that the tangential velocity component to the island, integrated around the island or ridge segment, must integrate to zero. So, for example, a long meridional island or ridge segment could not have motion in one direction along the ridge only on one side of the ridge in, say, the gravest meridional mode, without violating the circulation integral constraint. This forced such modes to have motion in both subbasins. The integral constraint is equivalent to the condition that the pressure perturbation on one side of the ridge can penetrate through the gap to excite motion in the other subbasin. Indeed, in PS we found two classes of free modes. In one class the meridional mode structure was even around the mid latitude of the basin. Such modes contain meridional velocities on the east side of the ridge that do not integrate to zero on that side alone and so excite full basin modes. Another class of modes were those that were antisymmetric about the mid latitude. Such modes are limited to one or the other of the subbasins and satisfy the integral constraint simply by having a meridional velocity that integrates to zero on the side of the island bounding the subbasin in which the mode is found. It is important to emphasize the crucial role of there being at least two gaps so that the segment is islandlike and Kelvin's theorem obtains. Were there a single gap, as discussed in Pedlosky and Spall (1999), the wave would be largely blocked.

Surprisingly, the normal mode frequencies for the full basin modes in the case of the thin meridional island were very close to the normal frequencies for the full basin without the barrier. Of course the frequencies for the subbasin modes were precisely those of the Rossby basin modes for the appropriate subbasin.

In the present study, we extend the results of PS by examining the case in which the island or ridge segment has a finite width and in which bottom friction and lateral friction are present. In particular, we examine the case in which lateral friction, strongly scale dependent, is important primarily in the gaps. We develop an analytical solution for the response of the fluid to a localized forcing in one subbasin at an arbitrary forcing frequency.

Of particular interest is the role of friction in the gaps in determining the degree to which variability, excited in one subbasin, will excite motion in the other. We shall show below that the transmission depends on the degree of friction in the gap, the width of the island (and so the gap length), and the spatial structure of the forcing. Much of this dependence can be understood in terms of the basic structure of the normal modes, even in those cases in which the friction is strong enough to eliminate any strong resonance with the modes. That is, the behavior of the forced response in the frictional case is well illuminated by the underlying structure of the inviscid normal modes described in PS.

In section 2 we develop the analytical solution for the forced problem. To keep matters as simple as possible a barotropic model is described, although it is not much more complicated to deal with the modes of a baroclinic model, each mode of which demonstrates similar behavior. The integral constraint is described and used as an important boundary condition to determine the flow through the gaps. In section 3 the basic solution is used to find the inviscid normal modes and in particular the dependence of the frequencies of the normal modes on the width of the island. In section 4 the response of the basin as a function of frequency is described. This is measured in terms of both the flow from one subbasin to the next, given by the island constant (described below) and the amplitude response at arbitrarily chosen points in each subbasin. Section 5 summarizes the results and discusses their significance.

It is important to emphasize that although the problem discussed here is presented in the context of the response of a closed basin to periodic forcing and the consequent possibility of resonance, the more fundamental issue it addresses is the transmission of large-scale Rossby wave energy through barriers that contain only small openings. As such, it relates to the general problem of transmission of planetary-scale energy in the deep ocean in the presence of midocean ridges or the possibility of similar transmission from one ocean basin to another across island arc chains, such as the Atlantic–Caribbean complex.

2. The forced problem

a. Model and solution

The basin and the island within it are shown in Fig. 1. The island is placed between longitudes x_1 and x_2 and in the meridional (y) direction leaves two channels of width d between the two subbasins of the overall basin. The containing basin lies between x_w and x_e. Additional gaps can be opened in the island but the added complexity, while of interest, can be intuited from the simple model described here. The meridional extent of the basin in dimensional units is L, which is used to scale lengths in the problem. Time is scaled by the characteristic Rossby wave period $(\beta L)^{-1}$.

The mathematical model for the flow that is employed is the linearized, quasigeostrophic vorticity equation (Pedlosky 1987) including lateral and bottom friction. In the scaled units described above, the equation is

$$\nabla^2\Psi_t + \Psi_x = -r\nabla^2\Psi + A\nabla^4\Psi + W(x, y, t). \quad (2.1)$$

In (2.1) Ψ is the streamfunction for the motion. The first term on the right-hand side of (2.1) represents the bottom friction and r can be thought of as the ratio of Stommel's boundary layer thickness to the basin scale L. The second term on the right-hand side of (2.1) is the lateral friction and in these nondimensional units it is the cube of the ratio of Munk's boundary layer thickness to L. We will consider both A and r as small parameters.

The last term on the right-hand side of the equation

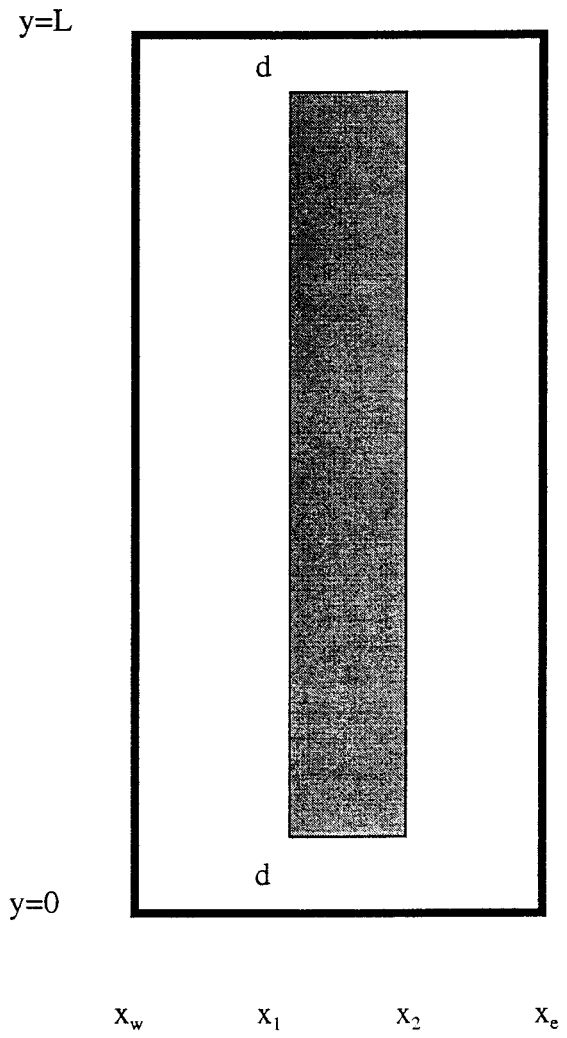

FIG. 1. A schematic of the oceanic basin with the island barrier. The barrier has the longitudinal extent $x_2 - x_1$ while the two gaps at the extreme edges of the island barrier have each width d. The basin has a meridional extent L. Shown in the figure are the coordinates of the features of the basin when scaled with the length L. A localized forcing is placed at $x = z$ with meridional structure described in the text.

is the external forcing. It is fundamentally a source of potential vorticity and within the context of quasigeostrophic dynamics it can be considered either as a wind stress curl or the vorticity source due to Ekman pumping. For abyssal flow it can be related to the upwelling from the abyss into the thermocline.

We will consider forcing harmonic in time so that

$$W = \mathrm{Re}[e^{i\omega_0 t} w(x, y)]. \tag{2.2a}$$

Solutions for Ψ will be sought in the form,

$$\Psi = \mathrm{Re}[e^{i\omega_0 t} \psi(x, y)], \tag{2.2b}$$

where ω_0 is the forcing frequency. The problem for ψ then becomes

$$i\omega \nabla^2 \psi + \psi_x = A\nabla^4 \psi + w(x, y). \tag{2.3}$$

In (2.3) the bottom friction has been included by defining

$$\omega = \omega_0 - ir. \tag{2.4}$$

Outside of the narrow gaps we shall ignore the effect of lateral friction. This will not allow us to satisfy no-slip (or no stress) conditions on the meridional boundaries of the island. If we were to include lateral friction, it would add a term of order $A^{1/2}$ to the solution for the streamfunction and only slightly alter the response of the fluid to the forcing. The major effect of the lateral friction occurs, rather, in the narrow gaps between the two subbasins where its role will be considered in detail. In the gaps the measure of lateral friction depends on the ratio of the Munk boundary layer width to the gap width; that is, if A_* is the dimensional lateral viscosity,

$$\delta_M / d = \left(\frac{A_*}{\beta}\right)^{1/3} \Big/ d, \tag{2.5}$$

which may be order unity.

On the exterior boundary of the basin the streamfunction must be spatially constant, and without loss of generality we set it equal to zero. On the island the streamfunction must also be spatially constant and it will harmonically oscillate in response to the external forcing. Its value gives us the instantaneous measure of the flux through the gaps. Thus, on the island,

$$\psi = \Psi_I. \tag{2.6}$$

The forcing will be represented in the meridional direction by the Fourier series:

$$w = \sum_{n=1} w_n(x) \sin(n\pi y). \tag{2.7}$$

In the regions *outside* the gaps, where lateral friction is neglected, a convenient representation of the solution for the streamfunction is

$$\psi = e^{ikx} \sum_{n=1} \phi_n(x) \sin(n\pi y), \tag{2.8}$$

where $k = 1/(2\omega)$ and where ϕ_n satisfies

$$\frac{d^2\phi_n}{dx^2} + a_n^2 \phi_n = \frac{w_n(x)}{i\omega} e^{-ikx}, \tag{2.9}$$

where $a_n^2 = k^2 - n^2\pi^2$.

The solution that we consider is one in response to a localized forcing in the right-hand subbasin. Obviously, the problem changes in only a trivial way if the forcing is in the left subbasin. We consider the forcing to be (spatially) a delta function in x located at $x = z$ so that

$$w_n = W_n \delta(x - z), \qquad x_2 < z < x_e. \tag{2.10}$$

The particular form of W_n will determine the meridional structure of the forcing, which we will leave ar-

bitrary for the moment. The solution of (2.9) is discussed in appendix A.

In the gaps the y scale of the solution shrinks so that y derivatives become more important than x derivatives. The dominant terms in (2.1) become in the gaps

$$i\omega\psi_{yy} - A\psi_{yyyy} = 0. \tag{2.11}$$

Note that the beta term is neglected in (2.11). The ratio of the beta term to the retained terms can be shown to be of order $A_*/\beta L^3 \ll 1$. Indeed for nondimensional frequencies of order unity, the y scale obtained from (2.11) is

$$\delta = \left(\frac{2A}{\omega}\right)^{1/2}. \tag{2.12}$$

This is just the boundary layer scale for the Stokes layer for a nonrotating fluid (Batchelor 1967) in which the balance is between the acceleration of the velocity tangent to the boundary and the frictional force along the boundary. The beta effect plays no role. However, since ω is (in dimensional units) of order βL, the relative importance of the beta effect and the frictional force in the gap is measured by $A_*/\beta L^3 \ll 1$.

The solution of (2.11) in the region between $y = 0$ (the southern boundary of the basin) and the southern boundary of the island is given by

$$\psi = A = By/d + C_1 \exp(\{1 + i\}y/\delta) + C_2 \exp(-\{1 + i\}y/\delta), \tag{2.13}$$

subject to the conditions:

$$\psi = 0, \qquad y = 0,$$
$$\psi = \Psi_I, \qquad y = d,$$
$$\psi_y = 0, \qquad y = 0, d. \tag{2.14}$$

The solution is completed in appendix B. It is clear from the statement of the problem that each of the constant coefficients in (2.13) will be proportional to Ψ_I. A similar solution in which $y \to 1 - y$ holds in the gap north of the island.

Thus along each of the longitudes of the island, x_1 and x_2, the streamfunction can be written as

$$\psi = \Psi_I g(y), \tag{2.15}$$

where in the latitude band of the island the function $g(y)$ is equal to unity, while in the gaps $g(y)$ is given by the solution (2.13). At these longitudes we require that the solutions of (2.9) and (2.11) be continuous. The details are given in appendices A and B.

The total solution is then given in terms of the external forcing amplitude, for example, W_n and the unknown streamfunction constant on the island, Ψ_I.

b. The integral constraint

The momentum equation consistent with (2.1) is

$$\frac{\partial \mathbf{u}}{\partial t} + \mathbf{k} \times \mathbf{u} = -\frac{\nabla p}{\rho} - r\mathbf{u} + A\nabla^2\mathbf{u} + \boldsymbol{\tau}/\rho, \tag{2.16}$$

where we have represented the forcing as a wind stress but we could equally well have considered the forcing as due to a source–sink flow appropriate to the abyss. We will assume that the stress has no component along the island boundary.

If the component of (2.16) tangent to the island is integrated around the island and if periodic motion is considered, as in the above analysis, we obtain as a fundamental integral constraint,

$$i\omega \oint_{C_I} \nabla\psi \cdot \mathbf{n}\, dl - A \oint_{C_I} \nabla\nabla^2\psi \cdot \mathbf{n}\, dl = 0, \tag{2.17}$$

where $\mathbf{n}$ is the unit normal vector to the island and we recall that ω includes the effect of bottom friction. The contour in (2.17) encircles the island on the contour C_I.

Since we have neglected lateral friction except in the gaps, the last term in (2.17) can be neglected along the contour except in the gaps where it must be considered. However, in the gaps, Eq. (2.11) implies that the terms in the solution (2.12) that reflect the structure of the frictional forces in the gap self-cancel in (2.17). Hence in applying (2.17) only the terms proportional to A and B in (B.1) enter and for them the last term in (2.17) is identically zero. Thus the integral constraint reduces to the statement that the first integral in (2.17) must itself satisfy the integral constraint in which the terms in C_1 and C_2 in (B.1) are not considered. This simplification leads to an equation relating the island constant Ψ_I and the forcing. After a little algebra, one obtains,

$$\Psi_I\left[\sum_{n=1} \mu_n g_n a_n \frac{\cos n\pi d}{n\pi} \frac{\sin a_n[L_x - l_x]}{\sin a_n(x_2 - x_e)\sin a_n(x_1 - x_w)} - 2\frac{(1 + q)l_x/d}{1 + q - \rho(1 - i)(1 - q)}\right] = -i\sum_{n=1} \mu_n \frac{W_n}{\omega n\pi} \cos n\pi d e^{ik(x_2 - z)} \frac{\sin a_n(z - x_e)}{\sin a_n(x_2 - x_e)}, \tag{2.18}$$

where the constants in (2.18) are given in appendices A and B. Here $L_x = x_e - x_w$ and $l_x = x_2 - x_1$ are the widths of the basin and island, respectively. Note that, since $\mu_n = 1 - (-1)^n$, the right-hand side of (2.18) is zero if W_n is zero for n odd. Thus, if the forcing is antisymmetric about the midlatitude of the basin, the right-hand side of (2.19) will vanish, which implies that Ψ_I will be zero in that case since the square bracket on the left-hand side cannot vanish for real ω_0 if friction is different from zero. Thus, antisymmetric forcing will not excite flow through the gaps. Such forcing will yield a response limited to the right-hand basin in which the forcing acts and the left-hand basin will remain at rest. For forcings that have an even component around the midlatitude; that is, if $W_n \neq 0$ for n odd, Ψ_I will be different from zero and motion will be excited in the other subbasin. This is precisely the symmetry character

of the global and subbasin normal modes previously found in PS.

3. The normal modes

Friction, especially in the gaps, will eliminate the possibility of perpetually oscillating normal modes. However, the structure and frequencies of the inviscid normal modes are useful pieces of information in helping to understand the response of the forced, viscous problem. The problem is discussed in detail in PS; here a brief description is given of the nature of the modes in the case when the island's width is not negligible. In particular, it is of interest to examine the dependence of the natural frequency of oscillation on the width of the island. To keep the discussion brief I will focus only on the gravest full basin mode. The higher modes are qualitatively similar. Of course, the frequencies of the subbasin modes are given by the standard formula:

$$\omega = \frac{1}{2\pi(n^2 + m^2/l_{sb}^2)^{1/2}}, \tag{3.1}$$

where l_{sb} is the zonal extent of the subbasin. For the full basin modes the dispersion relation, instead, follows from (2.19) if we set both the friction and the forcing to zero, in which case the dispersion relation is

$$\sum_{n=1} \mu_n^2 a_n \frac{\sin 2n\pi d}{n^3\pi^3 d} \frac{\sin a_n(L_x - l_x)}{\sin a_n(x_2 - x_e)\,\sin a_n(x_1 - x_w)} = 2l_x/d. \tag{3.2}$$

If the island becomes very thin so that terms l_x can be neglected even when compared with d, (3.2) becomes equal to the dispersion relation in PS. As shown in PS, there is a set of full basin normal modes. The frequency of these modes becomes smaller, the smaller the x scale of the normal mode. The gravest normal mode, in the case where $l_x \to 0$, has a frequency very close to the frequency of the normal mode, which would exist in the absence of the meridional barrier. The ''higher'' modes, with larger effective x wavenumber are even closer, numerically, to the barrier-free problem. It is therefore not surprising that in the present case the frequency of the basin-scale normal modes is reduced as the barrier island occupies a greater fraction of the total basin. Figure 2 shows the result of a calculation of the frequency of the gravest free mode of oscillation of the system as the barrier scale, l_x, increases. For this calculation the basin is square, that is, $x_e = 1$ while $x_w = 0$. From (3.2) it is clear that the frequency depends on l_x in a more complicated manner than just the ratio l_x/L_x but also on the positions of the boundaries of the island with respect to the outer boundaries of the basin. The quantitative character of the results in Fig. 2 will be altered slightly if the center of the island is moved from the position chosen for that calculation in which the midpoint is placed at $x = 0.5$. It has not been possible to find a simply understood representation of the behavior of the frequency on l_x, but the general reduction in the frequency is plausibly related to the decrease in the size of the fluid-containing region of the basin in a manner qualitatively, but definitely not quantitatively similar to that of (3.1). Snapshots of the mode at different points in its cycle are shown in Fig. 3 for the case where $l_x = 0.223$ and $\omega = 0.079\,687$. The structure of the gravest mode is closely related to the $n = 1$ Fourier mode, which is possible in the case of the barrier-free basin, although with the barrier all Fourier modes with n odd are required to represent the normal mode. On the other hand, the subbasin modes, are restricted to one or the other subbasins, and their gravest modes correspond to the $n = 2$ modes in (3.1). The $n = 1, 3, 5, \cdots$ modes in (3.1) are not allowed since they will not satisfy the integral condition (2.17). It is important to note the importance of the spatial structure of the modes in determining whether or not both subbasins are involved in the oscillation. We shall see that exactly this consideration enters the forced, dissipative problem.

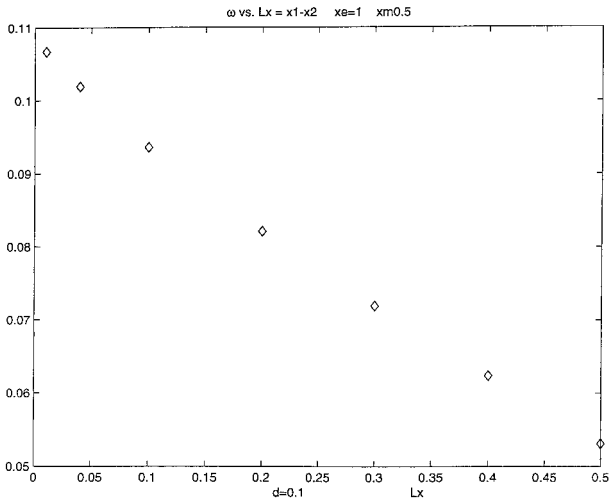

FIG. 2. The normal mode frequency of oscillation of the gravest Rossby normal mode as a function of island width.

For that problem we expect that the response in the basin across the island from the forcing will depend on both the spatial structure of the forcing and, with a dependence to be determined, also on the frequency of the forcing and the level of frictional dissipation.

4. Basin response

a. Forced response in the presence of friction

We use the solution (2.18) for the island constant Ψ_I and the solutions given in appendices A and B to discuss the response of the basin to a localized forcing placed in the right-hand subbasin. To fix ideas, the forcing is a delta function placed at $x = z = 0.8$ and the distribution in y is either a sharply peaked Gaussian-like distribution (whose Fourier amplitude is $W_n =$

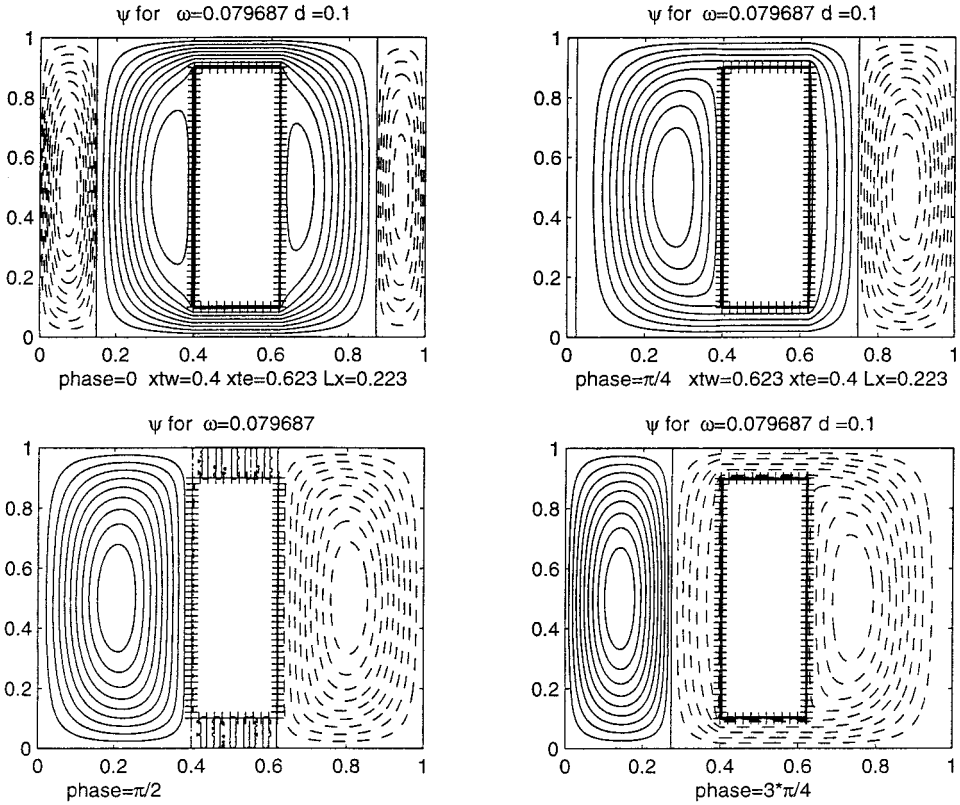

FIG. 3. The gravest basin-scale normal mode for the case $x_1 = 0.40$, $x_2 = 0.623$. In this calculation $d = 0.1$. The normal mode frequency (scaled by βL) is 0.079 687.

$2 \sin n\pi y_0 e^{-\kappa n^2}$, where y_0 is the central latitude of the forcing, while κ determines the narrowness of the forcing in y) or an antisymmetric forcing of two such Gaussians of opposite sign centered around the midlatitude of the basin for which $W_n = 2 \cos(n\pi/2) \sin n\pi\Delta y_0 e^{-\kappa n^2}$, where Δy_0 is the distance of each of the two peaks in the forcing from the midlatitude of the basin.

For the first forcing, if y_0 is at the midpoint of the basin, we would expect only solutions symmetric about the midlatitude to be excited. In view of our earlier discussions this would imply that the response will be of the full basin type. The subbasin modes require some component of the forcing to be asymmetric and would be absent if y_0 were ½. On the other hand, if the forcing were strictly antisymmetric, we would not expect the full basin modes to be excited and would anticipate that the variability would be restricted to the basin in which the forcing directly acts.

To discuss the response as a function of frequency for the several different forcings we examine both Ψ_I as a function of ω_0 and the amplitude at selected points in each of the two subbasins. For example, Fig. 4a shows the response for the amplitude at a point ($x = 0.6$, $y = 0.1667$) in the right-hand subbasin as well as the island constant for purely symmetric forcing, that is, for $y_0 = 0.5$. In this case the friction is very small. The bottom friction coefficient $r = 0.002$ and $\delta = 0.002$ while $d = 0.1$. Thus the lateral boundary layers occupy only a small portion of the gap (about 4%). Strong peaks in the response curves are seen at the normal mode frequencies for the full basin modes. In Fig. 4a the solid curve shows the amplitude response at the observation position while the dashed curve shows the response for the island constant. Note that for these modes the two curves peak at the same frequencies so that the local point response and the more global measure, given by Ψ_I, correspond. Figure 4b shows the response at a similarly, arbitrarily selected position in the left-hand basin, and we see that the response there peaks at the same frequencies. The strong response corresponds, at this low level of dissipation, with the full basin normal mode. Indeed, the contour plot of the response at the forcing frequency $\omega_0 = 0.104$ is shown in Fig. 4c. The resemblance to the normal mode shown in Fig. 3 is clear.

On the other hand, if the forcing is antisymmetric, the response curves are quite different. Figure 5 shows a response curve in such a case. The response in the right-hand basin, the subbasin where the forcing takes place, now resonates at only the subbasin normal mode frequencies; in this case the gravest subbasin mode has a frequency of about 0.0605. Note that Ψ_I is zero in this case. There is no communication between the subbasins, no fluid flux through the gaps in the island, and

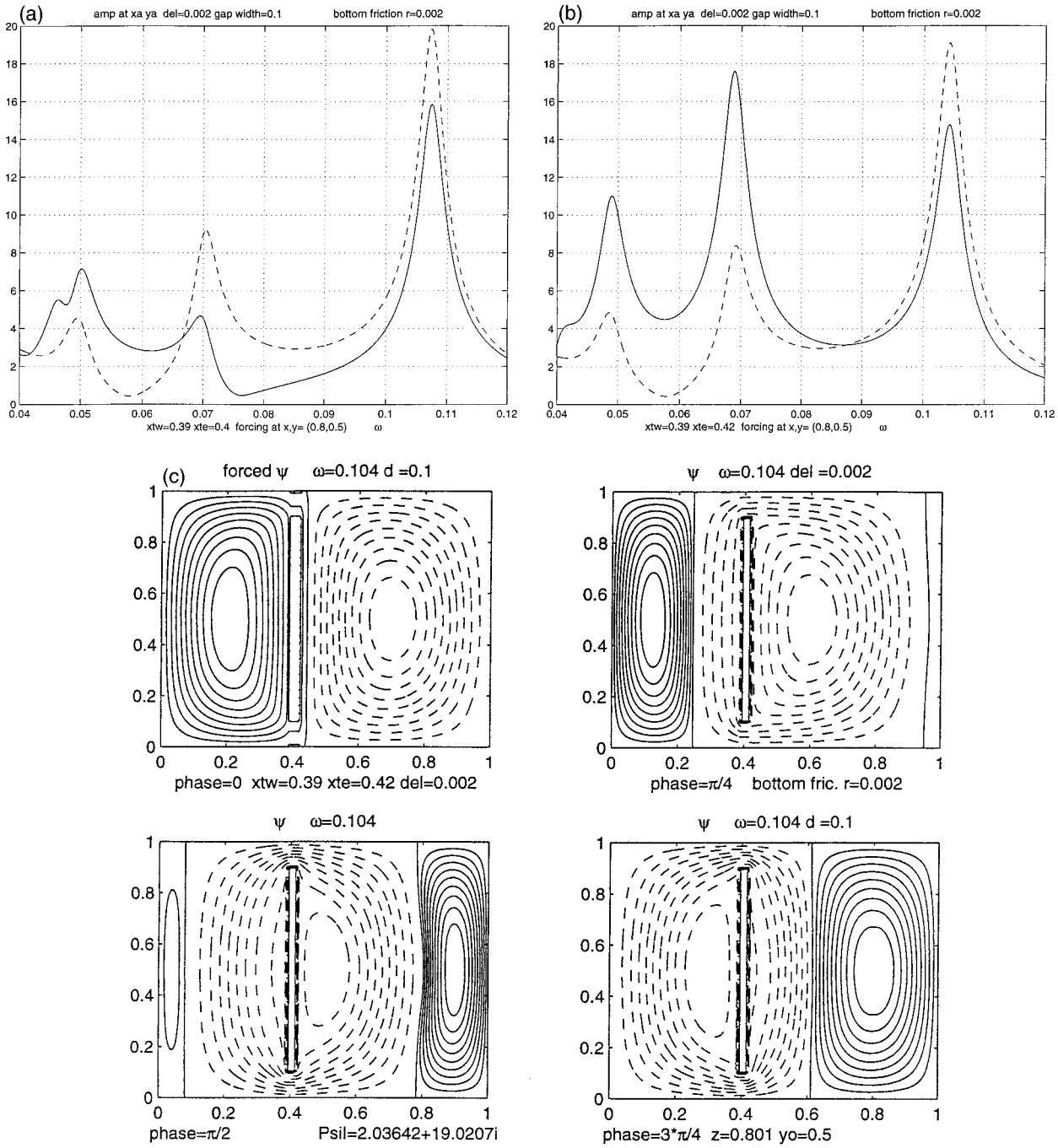

FIG. 4. The response of the fluid to symmetric forcing in the right-hand basin. The amplitude is measured at the point $x = 0.61$, $y = 0.1167$. The forcing is at $x = 0.8$. The frictional parameters are $r = 0.002$, $\delta = 0.002$; $x_1 = 0.39$, $x_2 = 0.42$. (a) The solid curve shows the amplitude of the response at the measuring point described while the dashed curve shows the modulus of the island constant Ψ_I. Note the coincidence of the peaks of the two curves. (b) As in (a) however measured in the left-hand subbasin at $x = 0.195$, $y = 0.5$. (c) Contour plots of the forced response at four phases of the oscillation cycle at frequency $\omega = 0.104$.

the response is limited to the right-hand basin almost entirely as shown in Fig. 5b, where the response is shown at the resonance frequency. This is a good example of how the basic structure of the normal modes helps determine the degree to which different forcings in one subbasin will excite a substantial response in the other subbasin. There must be substantial projection of the forcing on the full-basin normal mode structure for the disturbance to enter the other subbasin.

If the forcing is a mixture of symmetric and antisym-

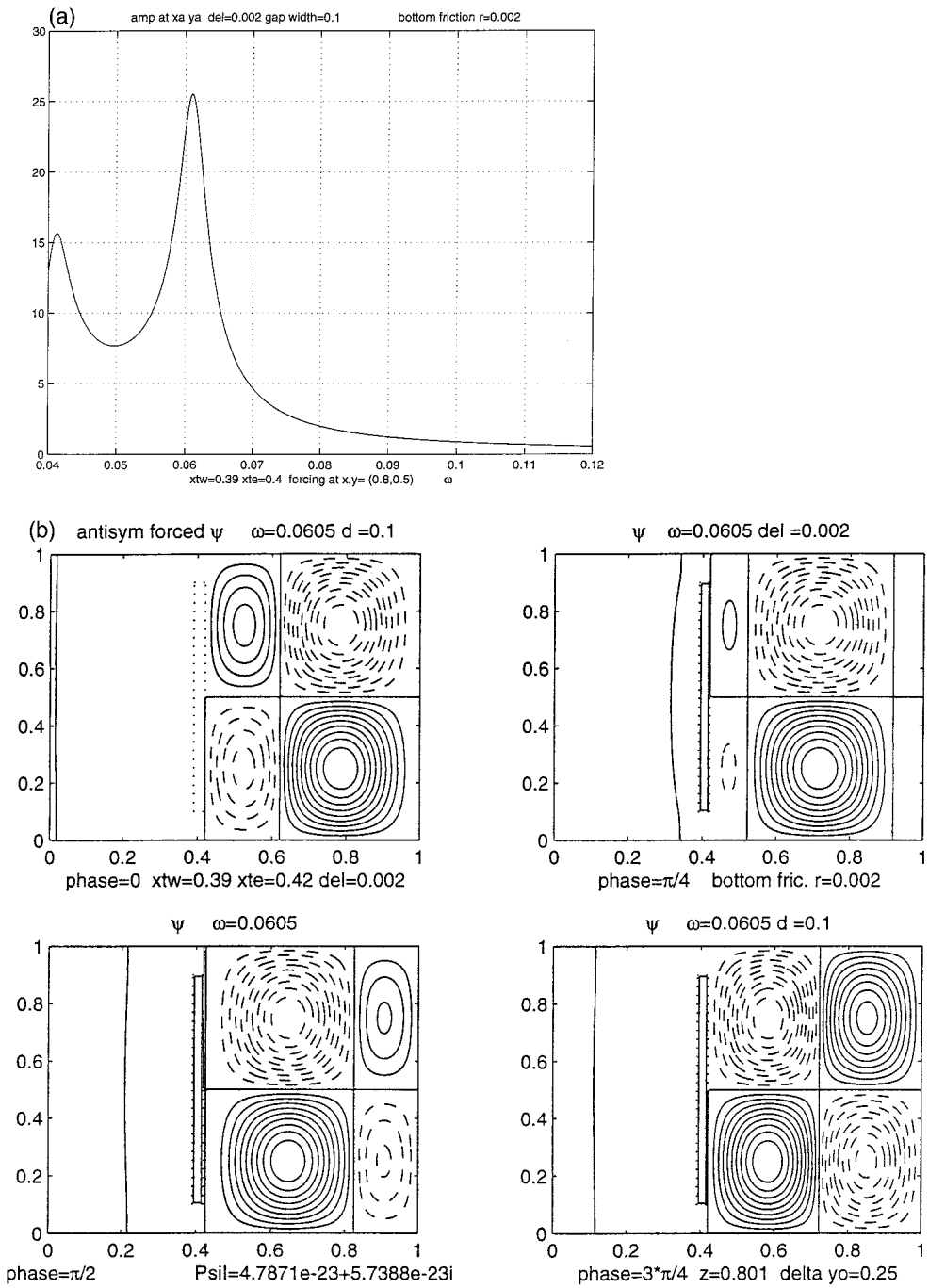

FIG. 5. For the same parameters as in Fig. 4 except that the forcing is antisymmetric around the midlatitude of the basin. (a) Amplitude in right-hand subbasin and the island constant. (b) Contour plot of the streamfunction at four phases of the oscillation.

metric parts, the response will contain both features. Figure 6a shows the response curves for the same parameter settings as in Figs. 4 and 5. The forcing is now the single-peaked Gaussian placed at $y_0 = 0.75$ so that it is asymmetric with both a symmetric and antisymmetric part. In Fig. 6a the response curve for the right-hand basin shows major peaks at the gravest full basin mode at $\omega = 0.104$, at which point the island constant also peaks, and a second major peak at the subbasin mode frequency where $\omega = 0.0605$. At this peak of the curve the response of the island constant has a minimum, reflecting the limitation of the response of this mode to the right-hand basin as was shown in Fig. 5b. At the particular location tested for response in the right-

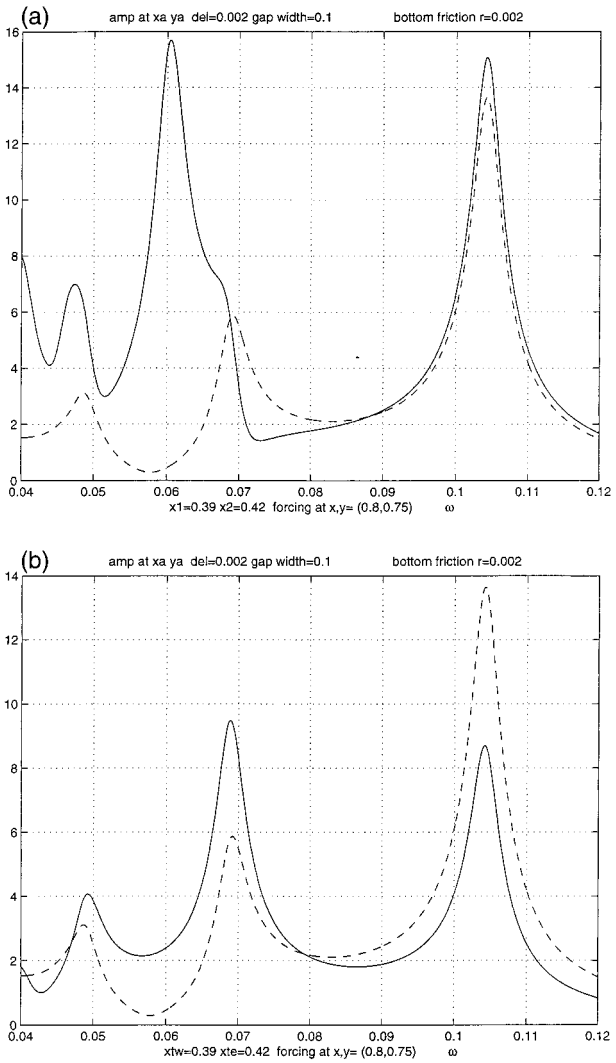

FIG. 6. As in Fig. 4 except that the forcing contains both symmetric and antisymmetric parts. (a) Response of amplitude in the right-hand subbasin and island constant. (b) Response in the left-hand subbasin.

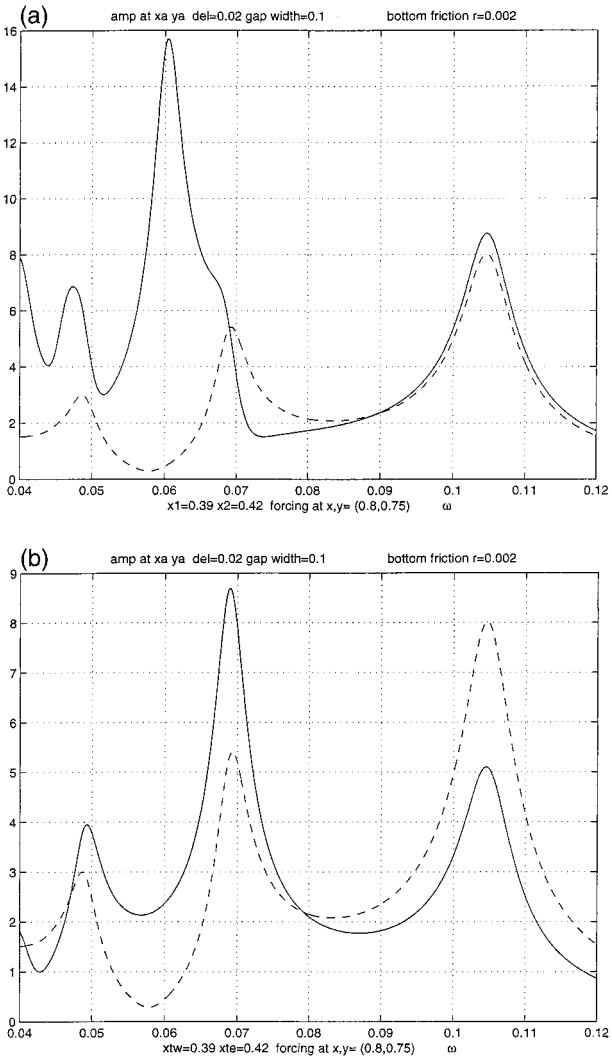

FIG. 7. As in Fig. 6 except the lateral friction has been increased so that now $\delta = 0.02$.

hand basin there is a hint, in the amplitude response, of another peak at the frequency of the second full basin mode at frequency $\omega = 0.07$. Note that Ψ_I has a clear peak at that frequency although the amplitude response is masked by the finite width of the larger peak at the subbasin mode. In Fig. 6b the response in the left-hand basin is illustrated. Here there are only *peaks at the full basin modes.* The subbasin mode does not provoke an oscillation in the left-hand basin and so there is no peak at $\omega = 0.0605$. In the left-hand basin the dominate peaks are the first and second full basin modes, and the amplitude response as a function of forcing frequency peaks in parallel with the peaks of the island constant.

Let us examine now how the response changes as we increase the friction in the gaps. Figure 7a shows the response curve if the lateral friction is increased by a factor of 100. This increases the boundary layer scale in the gap by a factor of 10 so that now the frictional boundary layers cover approximately 40% of the width of each of the two gaps ($\delta = 0.02$). Note that now the peak at the full basin mode is reduced over what was seen in Fig. 6a. The amplitude response is reduced by a factor of about ½, while the island constant is reduced by a similar factor. The standout peak is now the subbasin mode; however, it is interesting to see how robust the response at the full-basin mode frequency remains, even with such a large increase in the lateral mixing in the gap. Of course, the response in the left-hand basin is entirely dominated by the full basin mode, as is shown in Fig. 7b. All three peaks shown correspond to full basin normal modes. This is evident from the fact that each amplitude peak corresponds to a peak in the island constant Ψ_I and, of course, although the local amplitudes vary at the peaks from one subbasin to the other, the magnitude of the peaks for the island constant, being

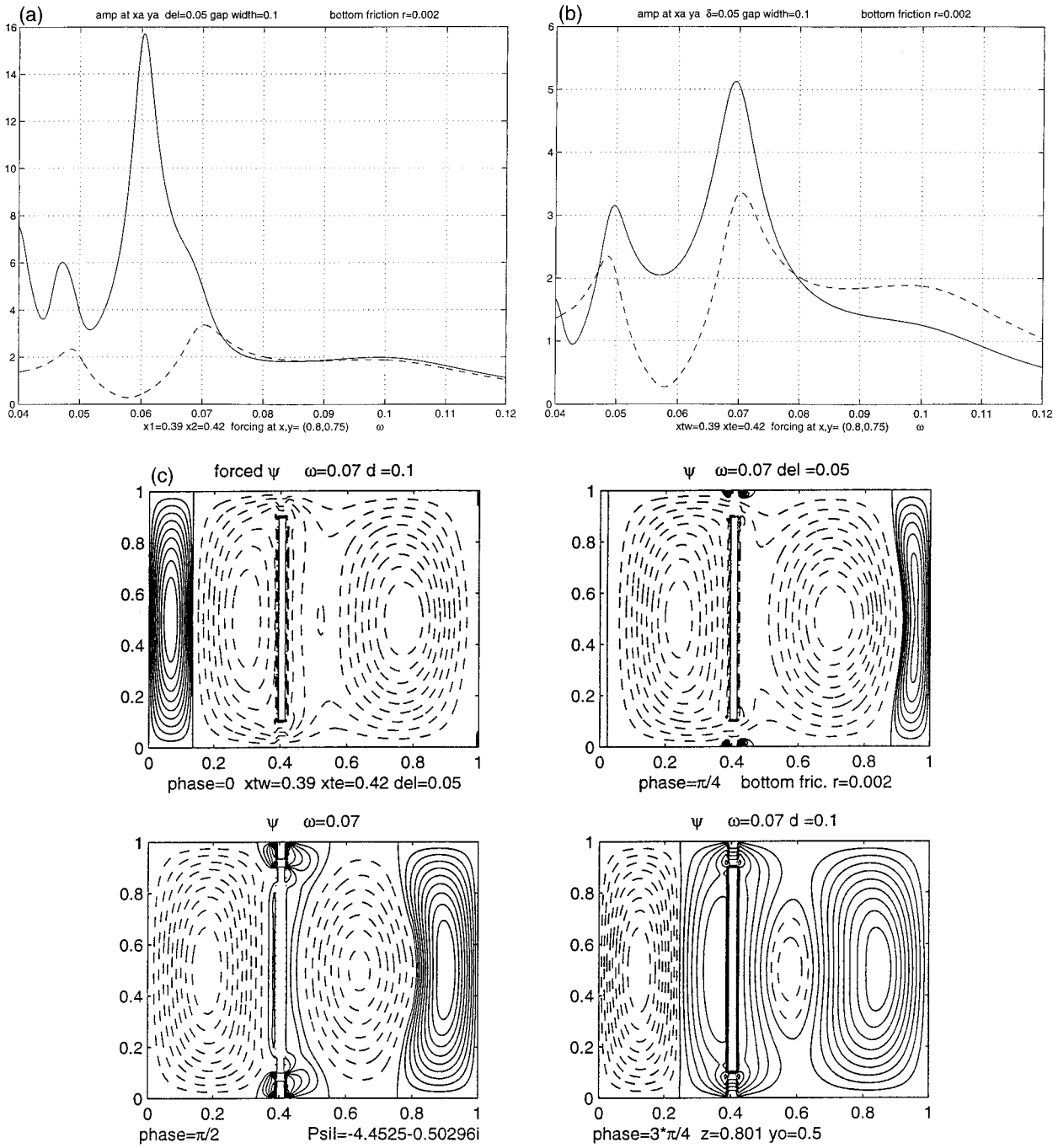

FIG. 8. As in Fig. 6 except the lateral friction is here such that $\delta = 0.05$. (a) Response in right-hand subbasin of amplitude at observation point and island constant. (b) Response in left-hand basin. (c) Contours of streamfunction for $\omega = 0.07$. (d) Contours of streamfunction for $\omega = 0.104$. (e) Contours of streamfunction for $\omega = 0.0605$.

basin rather than local quantities, are the same in both figures. Indeed, the correspondence between the peaks of amplitude and of Ψ_I is a rapid way of distinguishing the full basin modes.

For much larger values of δ the resonance at the full basin modes is no longer apparent. Figure 8a shows the response curve when $\delta = 0.05$ so that frictional effects will strongly affect the flow over the entire width of the gap. In this case a clear peak at the full basin mode is absent. There is a strong peak at the subbasin frequency (which we recognize because Ψ_I takes a dip there). There is another small peak at the full basin mode at $\omega = 0.070$, corresponding to the second normal mode in longitude. This peak shows up more clearly in the island

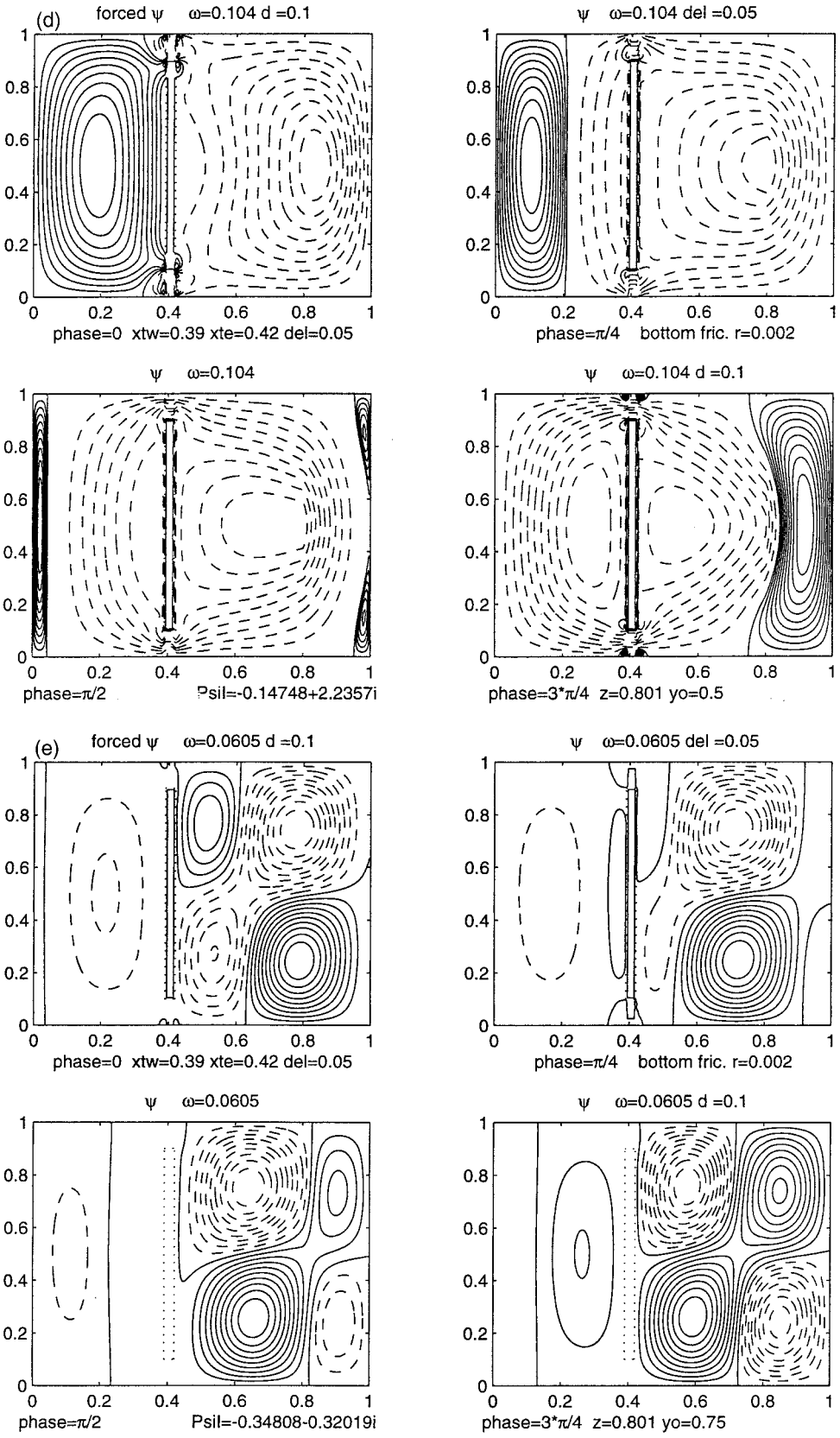

FIG. 8. (*Continued*)

constant than in the amplitude. The response at a point in the left-hand basin is shown in Fig. 8b. Here, of course, the large peak associated with the subbasin normal mode is absent and the response is dominated by the full-basin normal mode frequency at $\omega = 0.070$, whose island constant is greater than that of the gravest full basin mode. Figure 8c shows snapshots of the streamline contours for these values of the frictional parameters for a forcing frequency $\omega_0 = 0.07$ corresponding to the full basin mode with the largest island constant with this forcing. We see strong variability in both subbasins, as we would expect from Figs. 8a and 8b. Figure 8d shows contours of streamfunction at the same phase of oscillation as in 8c at the forcing frequency $\omega_0 = 0.104$, the frequency of the gravest normal mode of full basin type. As we saw, at this value of the dissipation, there is no peak in the response at the normal mode frequency. In the vicinity of the gravest normal mode frequency the response is essentially flat with frequency. Yet, when we examine the solution in Fig. 8d, there is a substantial signal in the left-hand basin. The forced variability squeezes through the gap, even in the absence of a resonance, and excites the entire basin. In this sense, the normal mode of full basin type can be seen to underlie the response of the forced, dissipative system even when the dissipation in the gaps is large enough to vitiate normal mode resonance. The response at those frequencies still resembles the normal modes. To emphasize the continuing importance of the normal modes, Fig. 8e shows the streamlines for the forced response at $\omega_0 = 0.0605$, near the resonance with the subbasin mode of the right-hand basin. The response is limited almost entirely to the right-hand basin so that once again the nature of the response in this case is explicable in terms of the underlying set of inviscid normal modes.

If the friction in the gap is increased still further, we reach a point where the gaps are essentially blocked by frictional forces. The island constant becomes very small, indicating very little communication between the two basins. For example, when $\delta = 0.5$ and $d = 0.1$, friction completely dominates in the gaps and the response is shown in Fig. 9 at a forcing frequency $\omega_0 = 0.08$, which corresponds to the peak in the island constant, Ψ_I. Now there is scarcely any transmission of disturbance energy into the left-hand basin.

If the effect of friction is increased everywhere in the basin by increasing the level of the bottom friction, the amplitude of the response will of course be reduced in the linear model. At the same time the sharpness of the resonance peaks of the response curves will also be reduced. Figure 10 shows the response curve for the island constant and the amplitude at the same point in the right-hand basin ($x = 0.61$, $y = 0.1667$) as well as the island constant for $r = 0.01$ and $\delta = 0.01$. We see that, as anticipated, both the amplitude and the sharpness of the peaks in both curves are reduced. At this value of bottom friction the Stommel boundary layer for the steady problem would occupy a little over 2% of the basin width. Even at this value, which might be considered a more realistic setting than the earlier cases with smaller r, the qualitative nature of the response curve is maintained and the streamfunction pattern, although not show here, is qualitatively similar to those displayed for smaller values of bottom friction.

As the island width increases, that is, as $l_x = x_2 - x_1$ is increased, the friction in the gap has a longer distance over which to operate. As we would expect, one effect of this is to reduce the efficiency of communication between the two basins by reducing the value of Ψ_I. Figure 11 shows the reduction of Ψ_I as a function of l_x. The gap length varies over an order of magnitude, but the island constant Ψ_I is only slightly reduced over this interval even though both the bottom friction and the lateral friction are substantial in this case ($r = 0.01$, $\delta = 0.01$). In order to choke off the gaps and eliminate the interbasin communication a very strong momentum dissipation is required as seen above.

b. *Response in the absence of a western reflecting boundary*

We have emphasized the role of inviscid normal modes in understanding the nature of the forced response of closed basins to localized forcings and the ability of large-scale variability to squeeze through narrow gaps in an otherwise impenetrable barrier to provoke strong variability in adjacent subbasins. In this section the response of a fluid is studied when the possibility of full basin resonance is completely removed. This can be done by eliminating the reflection of energy from the western boundary of the basin. We can think of this as either a semiinfinite basin in the zonal direction in which the barrier in our basin is so far removed from the western boundary that reflected energy cannot return to the barrier before it is dissipated or, more simply, that the western boundary layer region is a zone of complete absorption of energy. This can easily be done analytically by replacing the boundary condition of zero streamfunction at $x = x_w$ with a radiation condition there. Thus, west of the island barrier we insist that Rossby wave energy is propagating only westward. The details are described in appendix C.

We note from the form of Eq. (C.4) that a full basin, inviscid normal mode is no longer possible. There are no solutions of (C.4) for real frequency in the absence of forcing and dissipation for which Ψ_I is different from zero.

Figure 12 shows the response for Ψ_I as a function of frequency. In the absence of full-basin normal modes, the response curve is relatively flat. Only the phase of the island constant changes significantly as a function of frequency as shown by the relative size of the real and imaginary parts of Ψ_I shown in the figure. In the absence of the peaks the magnitude of the flux through the gaps as given by the island constant is reduced; still its mag-

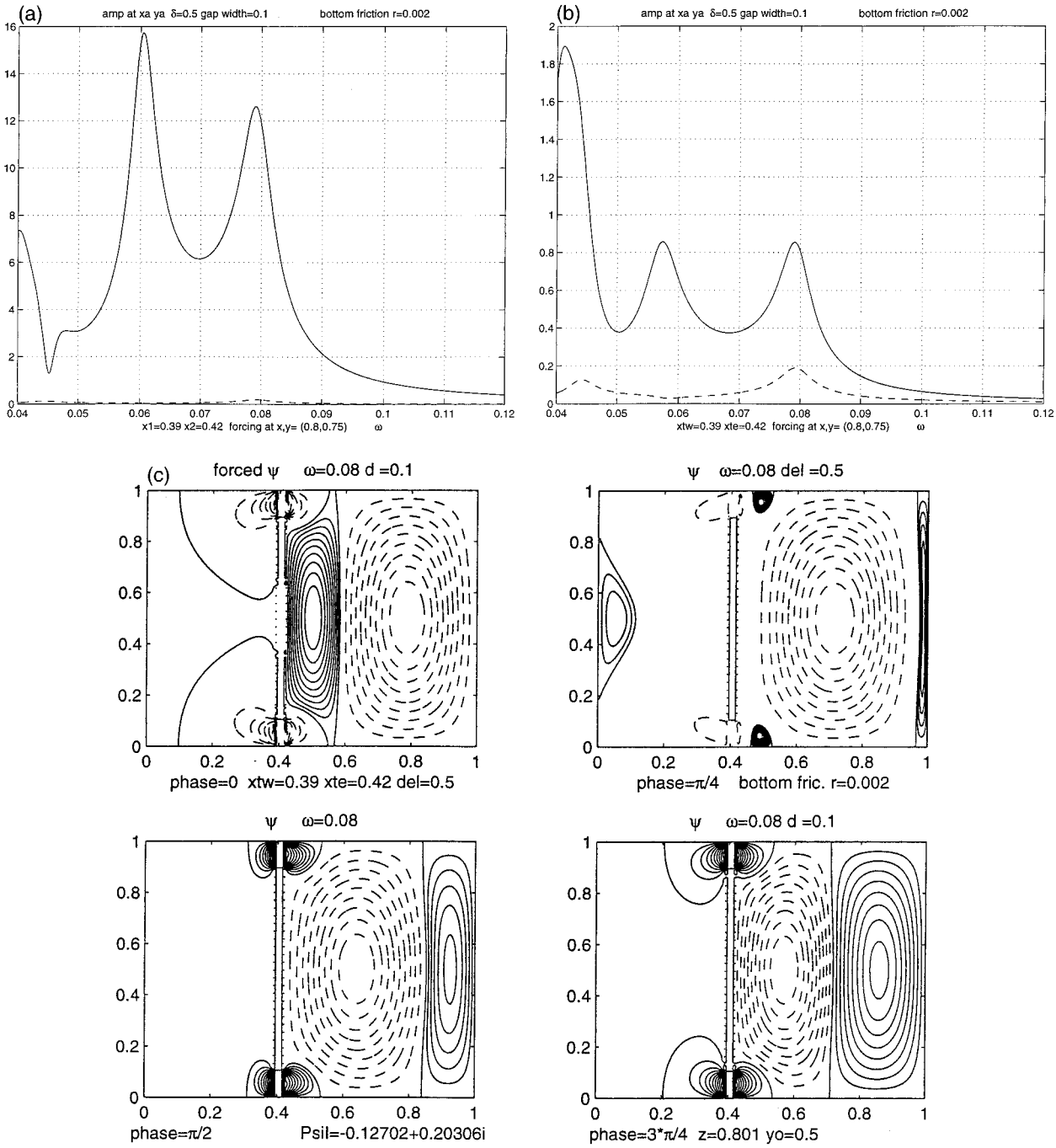

FIG. 9. As in Fig. 7 but now $\delta = 0.5$.

nitude is $O(1)$. Figure 13 shows snapshots of the forced oscillation, and we see that a substantial amount of the total variability is still able to penetrate the small gaps and excite the fluid to the west of the barrier. Clarke (1991) considered a related problem, that of the transmission of Kelvin and Rossby waves in the equatorial waveguide in the presence of blocking island barriers. Although he did not formulate his problem using the constraint (2.17), he reached similar conclusions about the ability of westward propagating waves to penetrate island barriers and, although his analysis relied strongly on certain properties of equatorial waves, there is fundamental agreement of this analysis with his conclusions.

5. Discussion and conclusions

We have examined here a simple model for the transmission of Rossby wave energy from one subbasin to

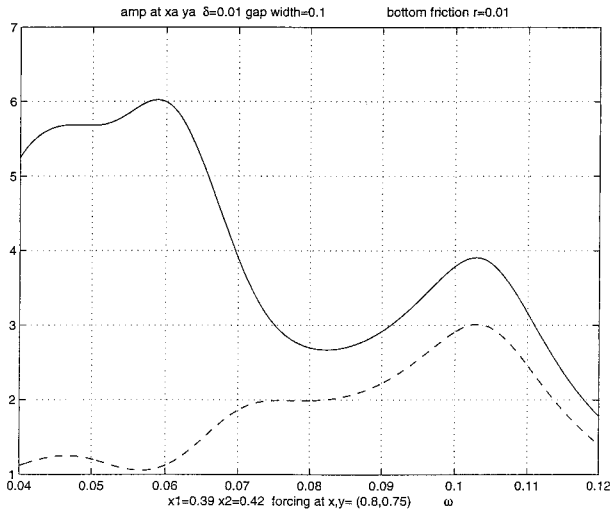

FIG. 10. The response curve in the right-hand basin for an increase in bottom friction. Here $r = 0.01$, $\delta = 0.01$.

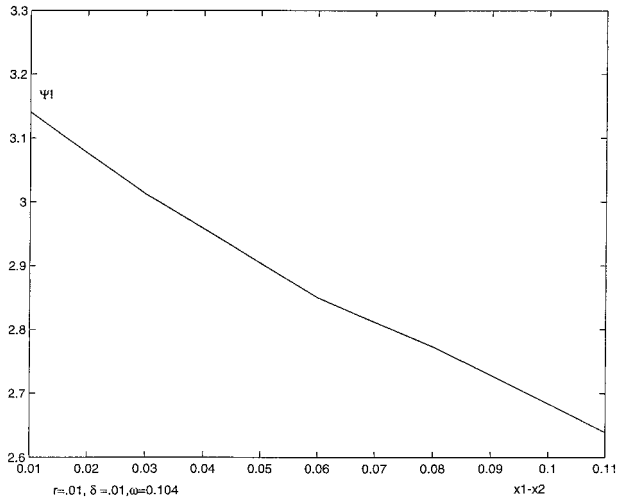

FIG. 11. The island constant Ψ_I as a function of island width for the frictional parameters of Fig. 10.

an adjacent subbasin when the two subbasins are separated by a barrier that nearly extends the meridional length of the total basin. The two subbasins are allowed to communicate only through very narrow gaps in which lateral mixing of momentum works to impede the propagation of energy. In addition, a background bottom friction mechanism acts everywhere in the basin to dissipate the energy introduced by the localized forcing. The model is presented as an idealized representation of the response of either the wind-driven circulation in the presence of large island barriers or the response of the deep abyssal circulation in the presence of midocean ridges. Although the simple model presented here has a prescribed forcing, the original motivation for the study came from the results of a numerical experiment of M. Spall (see PS for a discussion) in which the forcing is due to a localized, relatively small scale instability.

The results of the present study expand on the results of PS by considering the response of a forced, viscous fluid in the presence of a barrier island of nonzero width. The results described in section 4 show that even in the presence of substantial lateral friction acting in the gaps, the full basin will respond to localized forcing in one of the subbasins by responding globally. The nature of the response is both frequency and spatial-structure sensitive. When the forcing frequency corresponds to one of the subbasin normal modes, the response is largely limited to the basin in which the forcing occurs. When the frequency approaches a normal mode frequency of the total basin, the flux through the island/ridge gaps becomes large and the full basin responds strongly to the forcing. Increasing the level of the friction reduces the amplitude of the response and smears out the sharpness of the amplification as a function of frequency, but the overall qualitative behavior remains the same even for substantial friction in the gaps. The degree of penetration of disturbance energy from one subbasin to its neighbor is comprehensible in terms of the underlying inviscid normal mode structures.

When full basin resonance is eliminated by disallowing reflection from the basin's western boundary, the transmission of energy across the gap still qualitatively follows the pattern established by the normal mode resonance.

Underlying the question of the involvement of the adjacent basin to localized forcing is the application of the circulation integral constraint (2.17) around the island segment. This is a robust constraint, valid regardless of the level of nonlinearity. The requirement that modes containing tangential flow of largely a single sign along the island/ridge segment involve both subbasins is a direct consequence of the constraint. It is therefore to be expected that although the details of the response

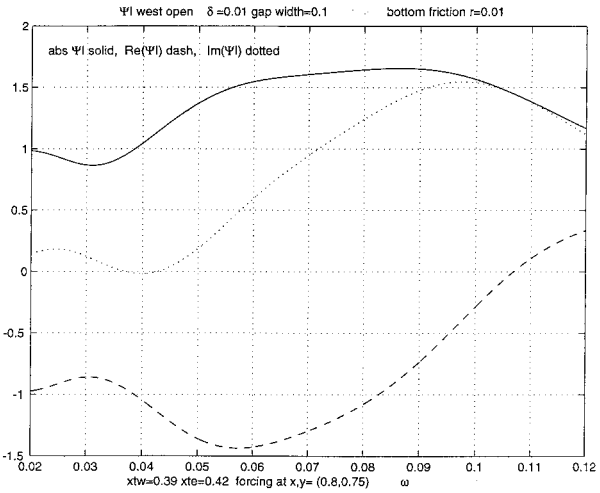

FIG. 12. The response curve for the island constant for the frictional parameters of Fig. 10 when the western boundary of the basin is nonreflecting.

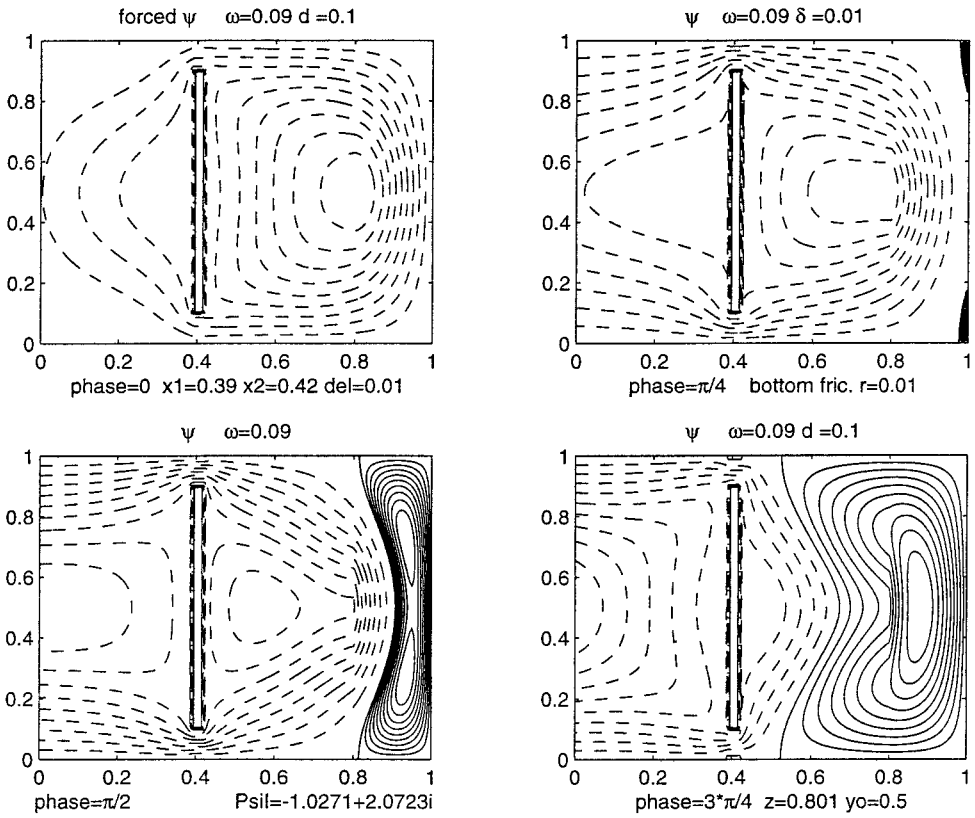

FIG. 13. The contours of the forced oscillation for the case shown in Fig. 12.

may alter as more realistic features of the model are added, the question of transmission of energy must ultimately deal with the physical consequences of the basic circulation constraint.

In this paper I have considered a ridge or island barrier with only two gaps at the extremes. As shown in PS, if new gaps are opened in the ridge, new full basin modes are allowed. It is anticipated then that, in the present model, the addition of further gaps in the island will allow more energy of higher meridional wavenumber to leak through the basin and involve the total basin in a coherent oscillation.

It will be interesting to examine the effects of nonlinearity, stratification, and more complex basinwide topography on the question of energy transmission. As discussed above, since the underlying constraint remains unchanged, an evolutionary alteration of the results can be expected.

Finally, I know of no direct field observations that speak to the issues raised here. It would be of interest to examine long-term records of variability in contiguous deep basins to search for coherence. At the same time, plans are afoot to examine the basic fluid mechanics of the process in the context of laboratory experiments.

Acknowledgments. I have had several interesting and helpful discussions about this problem with Michael Spall. This work has been supported in part by a grant from the National Science Foundation, OCE 9301845.

APPENDIX A

Solution of (2.9)

The solution of (2.9) is found separately in the three regions $x_w \le x \le x_1$, $x_2 \le x \le z$, and $z \le x \le x_e$. On x_w and x_e the streamfunction must be zero. On the longitudes x_1 and x_2 the streamfunction must be given by (2.15), where $g(y)$ or its Fourier transform is given below by Eq. (B.3). At $x = z$ the streamfunction must be continuous and, using (2.9) and (2.10), it follows that

$$\frac{d\phi_n(z_+)}{dx} - \frac{d\phi_n(z_-)}{dx} = -\frac{i}{\omega} W_n e^{-ikz}, \qquad \text{(A.1)}$$

where z_+ and z_- are the positions infinitesimally to the right and left of the point $x = z$.

Under these conditions the solution to (2.9) is easily found to be in $z \le x \le x_e$:

$$\phi_n = A_n^+ \frac{\sin a_n(x - x_e)}{\sin a_n(x_2 - x_e)}, \qquad \text{(A.2)}$$

while in $x_2 \le x \le z$:

$$\phi_n = A_n^- \frac{\sin a_n(x - x_e)}{\sin a_n(x_2 - x_e)} + B_n \frac{\cos a_n(x - x_e)}{\sin a_n(x_2 - x_e)}, \quad \text{(A.3)}$$

and in $x_w \le x \le x_1$:

$$\phi_n = D_n \frac{\sin a_n(x - x_w)}{\sin a_n(x_1 - x_w)}. \quad \text{(A.4)}$$

The coefficients are found by employing the boundary conditions described above and are

$$B_n = \frac{W_n}{i\omega a_n} e^{-ikz} \sin a_n(x_2 - x_e) \sin a_n(z - x_e), \quad \text{(A.5)}$$

$$A_n^- = \Psi_I g_n e^{-ikx_2} - \frac{W_n e^{-ikz}}{i\omega a_n} \cos a_n(x_2 - x_e) \sin a_n(z - x_e), \quad \text{(A.6)}$$

while

$$A_n^+ = A_n^- + B_n \cot a_n(z - x_2), \quad \text{(A.7)}$$

and where

$$g_n = 2 \int_0^1 g(y) \sin(n\pi y)\, dy, \quad \text{(A.8)}$$

where the function $g(y)$ is given in appendix B.

APPENDIX B

Solution in the Gaps

The coefficients in the solution (2.13) are determined by the boundary conditions (2.14). It follows that

$$A = -\Psi_I \frac{\rho(1 - q)}{(1 + i)[1 + q - \rho(1 - i)(1 - q)]}, \quad \text{(B.1a)}$$

$$B = \Psi_I \frac{(1 + q)}{[1 + q - \rho(1 - i)(1 - q)]}, \quad \text{(B.1b)}$$

$$C_1 = -\Psi_I \frac{q\rho}{(1 + i)[1 + q - \rho(1 - i)(1 - q)]}, \quad \text{(B.1c)}$$

$$C_2 = \Psi_I \frac{\rho}{(1 + i)[1 + q - \rho(1 - i)(1 - q)]}, \quad \text{(B.1d)}$$

where

$$\rho = \frac{\delta}{d}, \quad \text{(B.2a)}$$

$$q = e^{-(1+i)/\rho}. \quad \text{(B.2b)}$$

The key parameter here is ρ, which measures the characteristic y scale due to lateral friction, $(2A/\omega)^{1/2}$, against the gap width. This parameter is zero for an inviscid fluid and becomes order one as the lateral friction fills the gap. When this parameter is large, the geostrophic balance in the gap is affected by friction in the momentum equation. As we shall see, the effect of lateral friction becomes significant before this point is reached.

In the gap to the north, that is, in $1 - d \le y \le 1$, the same solution applies with y replaced by $1 - y$.

Along both $x = x_1$ and $x = x_2$ the streamfunction is given by $\psi = \Psi_I$ for $d \le y \le 1 - d$. In the gaps the solution is given by (2.13), also proportional to Ψ_I. This determines the function $g(y)$. The Fourier sine transform of $g(y)$ is then easily determined as

$$g_n = 2\mu_n \frac{\sin n\pi d}{n^2\pi^2 d} \frac{(1 + q)}{[1 + q - \rho(1 - i)(1 - q)]} \frac{2i}{(2i + n^2\pi^2\delta^2)} + 2\mu_n \frac{\rho(1 - q)(1 - i)}{n\pi[1 + q - \rho(1 - i)(1 - q)]} \times \left[-\frac{1}{2}(1 + \cos n\pi d) + \frac{n^2\pi^2\delta^2}{(2i + n^2\pi^2\delta^2)} \cos n\pi d \right], \quad \text{(B.3)}$$

where

$$\mu_n = 1 - (-1)^n.$$

In the limit $\rho \to 0$, g_n reduces to the simple formula found in PS in which it was assumed that the behavior of ψ was linear in the gap. Here, that behavior is derived exploiting the finite length of the channel and its narrowness as well as the uniform boundary conditions along the channel.

APPENDIX C

Solution for Open Western Boundary

When the western boundary at $x = x_w$ is rendered open, the solution of (A.1) in the western subbasin becomes

$$\psi = e^{i\omega_0 t} \sum_{n=1} \psi_n(x) \sin n\pi y, \quad \text{(C.1)}$$

where now

$$\psi_n = A_n e^{im_n(x - x_1)}, \quad \text{(C.2a)}$$

$$m_n = \frac{1}{2\omega} - \frac{1}{2\omega}[1 - 4n^2\pi^2\omega^2]^{1/2}. \quad \text{(C.2b)}$$

It is easy to check that the effect of bottom friction, which renders ω complex, produces an exponential decay of the solution *westward* from the barrier. Or, equivalently, for very small bottom friction the choice of sign in (C.2b) is equivalent to choosing the long Rossby wave whose zonal energy flux is westward. Again, using the results of appendix B, the coefficient A_n can be determined by matching the streamfunction to its value at the longitude of the barrier; hence,

$$A_n = \Psi_I g_n, \quad \text{(C.3)}$$

where g_n is given by (B.3). Application of the integral constraint (2.17) again yields an expression for the island constant, Ψ_I; thus, instead of (2.19) we now obtain

$$\Psi_I\left[\sum_{n=1} g_n \cos n\pi d \frac{a_n}{n\pi}\{i + \cot a_n(x_2 - x_e)\} - \frac{2(1 + q)l_x/d}{1 + q - \rho(1 - i)(1 - q)}\right] = -i \sum_{n=1} \frac{\mu_n W_n}{\omega n\pi} \cos n\pi d \frac{\sin a_n(z - x_e)}{\sin a_n(x_2 - x_e)} e^{ik(x_2 - z)}, \tag{C.4}$$

which completes the solution.

REFERENCES

Batchelor, G. K., 1967: *Introduction to Fluid Mechanics.* Cambridge University Press, 615 pp.

Clarke, A. J., 1991: On the reflection and transmission of low-frequency energy at the irregular western Pacific Ocean boundary. *J. Geophys. Res.,* **96** (Suppl.), 3289–3305.

Pedlosky, J., 1987: *Geophysical Fluid Dynamics.* Springer-Verlag, 710 pp.

——, and M. A. Spall, 1999: Rossby normal modes in basins with barriers. *J. Phys. Oceanogr.,* **29,** 2332–2349.

——, L. J. Pratt, M. A. Spall, and K. R. Helfrich, 1998: Circulation around islands and ridges. *J. Mar. Res.,* **55,** 1199–1251.